

The contribution of wildfire to PM_{2.5} trends in the USA

<https://doi.org/10.1038/s41586-023-06522-6>

Received: 5 January 2023

Accepted: 7 August 2023



Check for updates

Marshall Burke^{1,2,3,7}✉, Marissa L. Childs^{4,7}, Brandon de la Cuesta², Minghao Qiu⁵, Jessica Li², Carlos F. Gould⁵, Sam Heft-Neal² & Michael Wara^{1,6}

Steady improvements in ambient air quality in the USA over the past several decades, in part a result of public policy^{1,2}, have led to public health benefits^{1–4}. However, recent trends in ambient concentrations of particulate matter with diameters less than 2.5 μm (PM_{2.5}), a pollutant regulated under the Clean Air Act¹, have stagnated or begun to reverse throughout much of the USA⁵. Here we use a combination of ground- and satellite-based air pollution data from 2000 to 2022 to quantify the contribution of wildfire smoke to these PM_{2.5} trends. We find that since at least 2016, wildfire smoke has influenced trends in average annual PM_{2.5} concentrations in nearly three-quarters of states in the contiguous USA, eroding about 25% of previous multi-decadal progress in reducing PM_{2.5} concentrations on average in those states, equivalent to 4 years of air quality progress, and more than 50% in many western states. Smoke influence on trends in the number of days with extreme PM_{2.5} concentrations is detectable by 2011, but the influence can be detected primarily in western and mid-western states. Wildfire-driven increases in ambient PM_{2.5} concentrations are unregulated under current air pollution law⁶ and, in the absence of further interventions, we show that the contribution of wildfire to regional and national air quality trends is likely to grow as the climate continues to warm.

The observed multi-decadal decline in ambient air pollutant concentrations across the USA has been widely celebrated, both for its demonstrated human health benefits and because it was substantially a result of bipartisan public policy choices: in particular the Clean Air Act and its amendments^{1–3}. Recent data, however, indicate that these air quality gains are stagnating or even reversing across nearly all of the USA (Fig. 1), raising questions about whether past progress is being durably undone, what is causing this and if or how policy should respond.

Here we study the contribution of growing wildfire activity to recent trends in concentrations of ambient particulate matter with diameters less than 2.5 μm (PM_{2.5}). Wildfires have increased in size and severity in recent years, a consequence of a changing climate that has made fuels more arid and flammable and resulting fires larger and more severe^{7–9}, a century of fire suppression in western forests that contributed to fuel abundance¹⁰ and an increase in fire ignitions caused by humans¹¹. Increased fire activity has in turn led to increases in the emission and formulation of many air pollutants, including ‘criteria’ pollutants such as PM_{2.5}. These pollutants are regulated in the USA under the Clean Air Act and have been shown to have a wide array of negative health effects¹². Studies using data from before 2016 concluded that the wildfire contribution to measured PM_{2.5} concentrations was apparent mainly in the northwest of the contiguous USA (CONUS), but disagreed over whether enhancements in this region were observable in average annual concentrations or only in extreme daily concentrations^{13,14}. Studies that include more recent data from the very active 2018 and/or 2020 wildfire seasons

conclude that the imprint of wildfire smoke on surface average and extreme PM_{2.5} concentrations has expanded substantially in geographic scope, with observed enhancements throughout much of the western USA^{5,15,16}. Research also suggests that wildfire smoke is increasingly implicated in ‘exceptional event’ designations, or days on which regulators exempt observed pollutant concentrations from determination of regulatory attainment under the Clean Air Act because the source of the pollution was deemed beyond control of local authorities¹⁷.

Yet wildfires are clearly not the only possible contributor to recent air quality trends. A large body of work shows how changes in methods of production in the energy, manufacturing and other industrial sectors, in agricultural production practices, in regulatory enforcement and changes in global trade patterns have shaped short- and long-term variation in air pollution concentrations throughout the USA^{5,18–20}. Accurate and up-to-date characterization of the drivers of recent air quality trends is important to inform policy decisions about how to regulate or improve air quality, and whether interventions should be targeted to specific regions or sectors.

To isolate the contribution of wildfire smoke to pollution concentrations, we build on earlier work^{14,16} and use a combination of ground- and satellite-based measurements to isolate the component of surface PM_{2.5} concentrations attributable to wildfire smoke. Specifically, our primary analysis combines daily data from thousands of regulatory pollution monitoring stations from across the USA with satellite- and analyst-based estimates of when and where wildfire smoke is in the air

¹Doerr School of Sustainability, Stanford University, Stanford, CA, USA. ²Center on Food Security and the Environment, Stanford University, Stanford, CA, USA. ³National Bureau of Economic Research, Cambridge, MA, USA. ⁴Center for the Environment, Harvard University, Cambridge, MA, USA. ⁵Department of Earth System Science, Stanford University, Stanford, CA, USA. ⁶Woods Institute of the Environment, Stanford University, Stanford, CA, USA. ⁷These authors contributed equally: Marshall Burke, Marissa L. Childs. ✉e-mail: mburke@stanford.edu

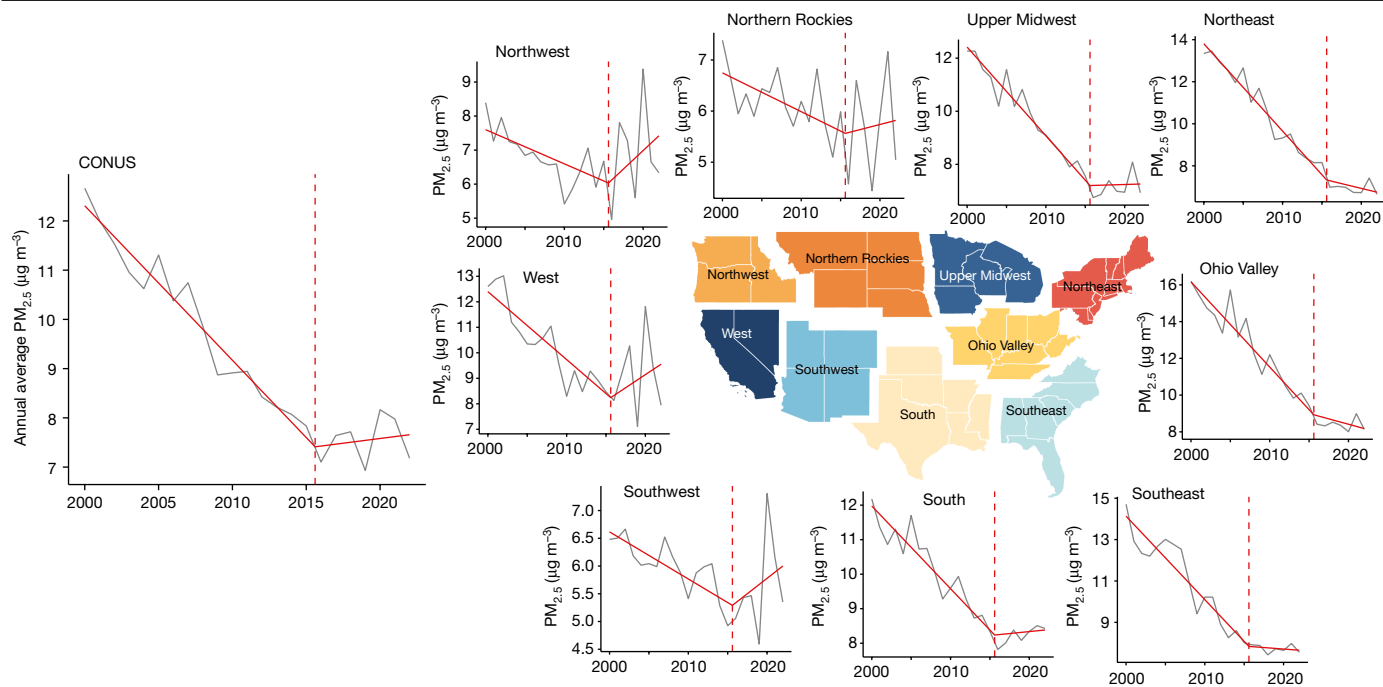


Fig. 1 | National and regional trends in ambient concentrations of $PM_{2.5}$ show steady declines through 2016 and then stagnation or reversal. Grey lines in each subplot are annual average regional or CONUS concentrations of $PM_{2.5}$ averaged over monitoring stations reporting consistently over the period in each US climate region^{32,33}. Regional and national averages are computed

from monitoring stations reporting over 50 days per year for at least 15 years to prevent station intermittency from influencing trends. Red lines are linear fits to each region’s annual average time series, with separate slopes fits for before and after the series breakpoint, denoted as the red vertical dotted line.

(Extended Data Fig. 1). To analyse trends in total $PM_{2.5}$, we use monitoring data from 2000 to 2022. We analyse the smoke contribution to total $PM_{2.5}$ beginning in 2006, when smoke plume data become available. To estimate smoke $PM_{2.5}$ over the 2006–2022 period, we calculate daily $PM_{2.5}$ anomalies from season- and time period-specific median concentrations at each location and attribute these anomalies to wildfire if satellite images indicate a wildfire plume is overhead on a given day (Methods). For this approach to successfully isolate wildfire’s contribution to surface $PM_{2.5}$, it must be the case that satellite-derived plume estimates accurately describe the location of wildfire smoke, and that the presence or absence of a plume is not systematically correlated with other non-wildfire sources of variation in surface $PM_{2.5}$. Using measurement data on the chemical components of $PM_{2.5}$ and panel regression, ref. 16 shows that both these conditions are likely to hold. Non-wildfire $PM_{2.5}$ on a given day can then be calculated as the difference between total observed and wildfire-attributed $PM_{2.5}$. Total, wildfire or non-wildfire $PM_{2.5}$ can be spatially or temporally aggregated to characterize wildfire’s contribution to average or extreme daily $PM_{2.5}$ concentrations. We focus on two measures of ambient air quality: annual average $PM_{2.5}$ concentrations, calculated as the simple average of daily $PM_{2.5}$ concentrations at a given station in a year, and the proportion of days above $35 \mu\text{g m}^{-3}$ at each station over 1 year, a concentration threshold used at present as part of Clean Air Act attainment designations.

To characterize trends in total or non-smoke $PM_{2.5}$ averages and extremes, and to test whether trends in each have changed over time, we use formal tests to identify trend breaks to divide our sample into ‘early’ and ‘recent’ periods²¹, estimate trends in pollutant concentrations in each period and then test whether trends are statistically different ($P < 0.05$) between the two periods, propagating uncertainty in both the trend break and the estimated slopes using a bootstrap procedure (Methods). CONUS-wide data indicate a trend break around 2016 (median estimate 2015.6) for annual average $PM_{2.5}$, and in 2012 (median estimate 2011.99) for extreme daily $PM_{2.5}$, consistent with visual evidence (Fig. 1 and Extended Data Figs. 2 and 3).

To test whether trends in average or extreme $PM_{2.5}$ are different between periods, we fit linear panel regressions to all stations in each geographic region of interest in each period (typically, state), allowing average pollution levels to differ across stations but estimating a common trend across all stations (Methods). Using total $PM_{2.5}$, we identify ‘reversals’, states in which $PM_{2.5}$ was declining in the early period but increasing in the recent period ($P < 0.05$), or ‘stagnations’, states where trends in total $PM_{2.5}$ were slower in the recent period but either still declining or not significantly increasing. Then using our measures of smoke $PM_{2.5}$, we identify ‘smoke-influenced’ regions as those where recent-period trends in total $PM_{2.5}$ were statistically distinguishable from trends in non-smoke $PM_{2.5}$ (Methods and Extended Data Table 1).

We test robustness to alternate statistical approaches to estimating pollution trends on either side of the break, to exclusion of recent extreme wildfire years and to different ways of constructing the smoke $PM_{2.5}$ data. Because individual stations come online at different times and report at different daily frequencies, we also test robustness to sample restrictions that limit stations to those reporting more frequently and/or reporting for fewer years in the sample (Methods). Finally, we note that trends in a state or region’s $PM_{2.5}$ concentrations need not necessarily reflect trends in that region’s emissions of particulates and their precursors, given that wildfire smoke often travels long distances²².

In 41 out of 48 states in CONUS, average annual $PM_{2.5}$ concentrations were declining over the early period (2000 to roughly 2016, depending on bootstrap run) but then either significantly slowed (30 ‘stagnating’ states) or began to reverse (11 ‘reversing’ states) (Fig. 2a). In the remaining seven states, either early trends were not declining, trends were not statistically different between early and recent periods, or declines accelerated between periods.

We find that wildfire smoke statistically significantly influenced recent trends in annual average total $PM_{2.5}$ in 35 states, representing 73% of all CONUS states. Pooling across all smoke-influenced CONUS states, we calculate that since about 2016, smoke has added an average of $0.69 \mu\text{g m}^{-3}$ to $PM_{2.5}$ concentrations (95% confidence interval:

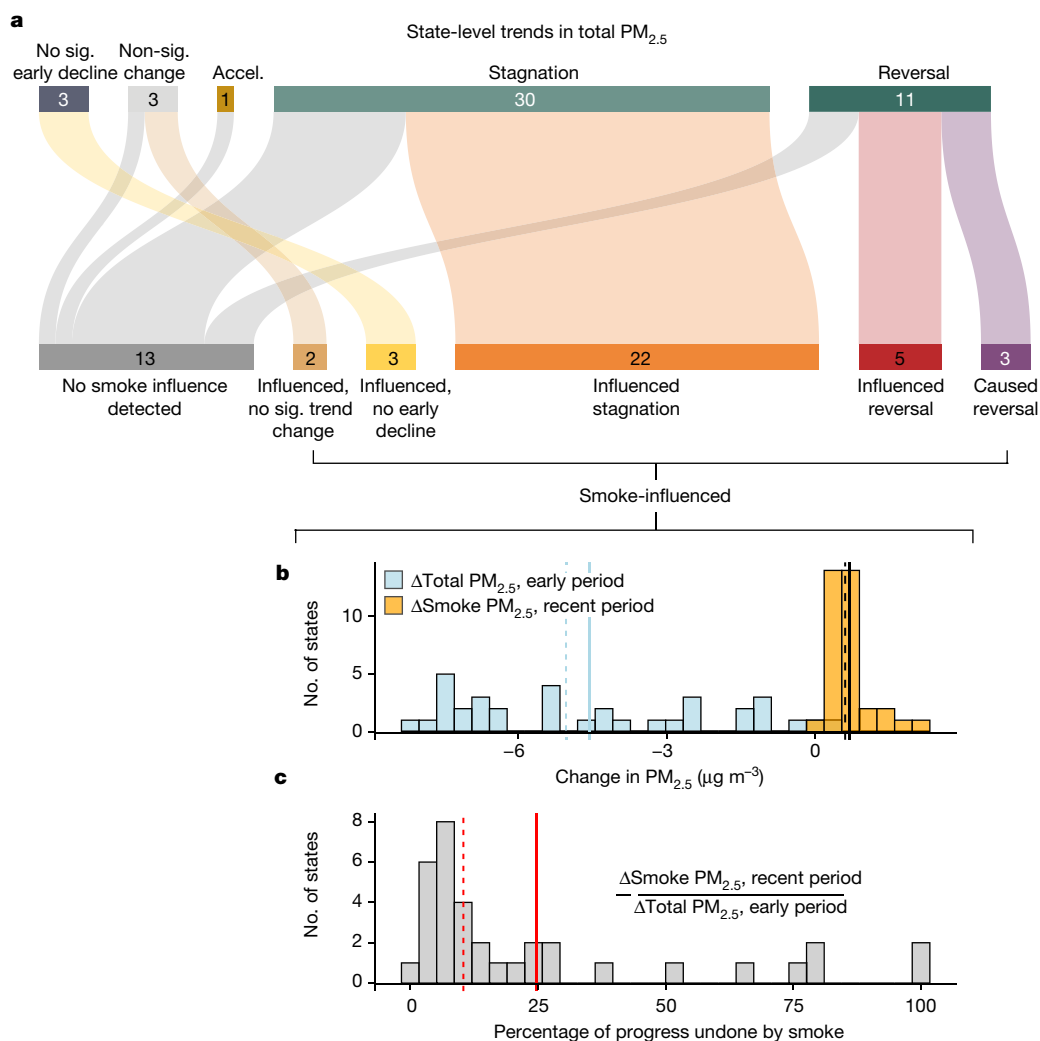


Fig. 2 | Improvements in total PM_{2.5} have slowed or reversed in most states, and smoke is a significant influence in most. **a**, Classification of states by trend in annual average total PM_{2.5} in the early (2000 to roughly 2016) versus the recent period (roughly 2016 to 2022); non-declining are states where early-period PM_{2.5} is not declining ('no sig. early decline') or where trends in early and recent periods are not statistically different ('non-sig. change'). 'Stagnation' includes states where declines are slower ($P < 0.05$) in the recent period relative to the early period but not statistically significantly negative, 'reversal' includes states where the early trend was significantly negative and the recent trend was significantly positive, and accelerating ('accel.') includes states where the recent declines are faster than the early period. Numbers indicate states in each category, out of 48 CONUS states. An alluvial plot then

shows the count of states in each of these categories that are smoke influenced in the recent period, defined as total PM_{2.5} having a statistically significant steeper slope ($P < 0.05$) than estimated non-smoke PM_{2.5}. A 'caused reversal' is a recent-period trend in total PM_{2.5} that would have been negative absent smoke. **b**, In the 35 smoke-influenced states, the distribution of change in total PM_{2.5} during the early period (blue) and change in smoke PM_{2.5} during the recent period (orange). Dotted lines are medians across states and solid lines are means. **c**, Ratio of recent-period smoke-attributed PM_{2.5} increase to early-period total PM_{2.5} decline, representing the percent of early-period progress in reducing total PM_{2.5} concentrations that was undone by smoke in the recent period; the dotted red line is the median across states and the solid line is the mean.

0.64–0.74) (median 0.60 μg m⁻³ (0.52–0.67)), equivalent to 25% (20–29%) of the average decline in annual PM_{2.5} achieved in these states between 2000 and 2016 (median 10% (8–14%)).

In 22 of these 35 states, PM_{2.5} was still declining or flat in the recent period but would have declined faster absent smoke. These states are located throughout much of the US mid-west, south and east (Fig. 3). We calculate that since 2016, smoke added 0.47 μg m⁻³ (0.39–0.56) to annual PM_{2.5} concentrations in these 22 states (median), equivalent to 7% (6–8%) of the PM_{2.5} declines achieved in these states between 2000 and 2016, or median 1.1 (0.9–1.3) years of progress during those years (Fig. 2b,c).

In eight other states, total PM_{2.5} was trending significantly up since 2016 but would have either trended up more slowly (five states) or would have actually trended down (three states) absent smoke. These states are concentrated in the west and mid-west of the USA, and we calculate that smoke added 0.97 μg m⁻³ (0.85–1.08) to PM_{2.5} concentrations in

these states since 2016, equivalent to 46% (36–58%) of the median decline in annual PM_{2.5} achieved in these states between 2000 and 2016, or 7.1 (5.6–9.0) years of progress during that period. The remainder of states either had no detectable smoke influence in the recent period, such as many states in the northeast, or were smoke influenced in the recent period but did not have PM_{2.5} trending down in the early period or did not have a detectable change in PM_{2.5} trends, such as several states in the northern Rockies.

We emphasize that our measure of 'influence' is in regard to pollution trends rather than pollution levels, and that most western states have had substantial amplification of pollution levels due to wildfire smoke in certain recent years¹⁶, even if influence on trends is sometimes less apparent in certain locations (for example, South Dakota).

State-level estimates of pollution trends and their categorization regarding stagnating and/or reversing and smoke influence are largely

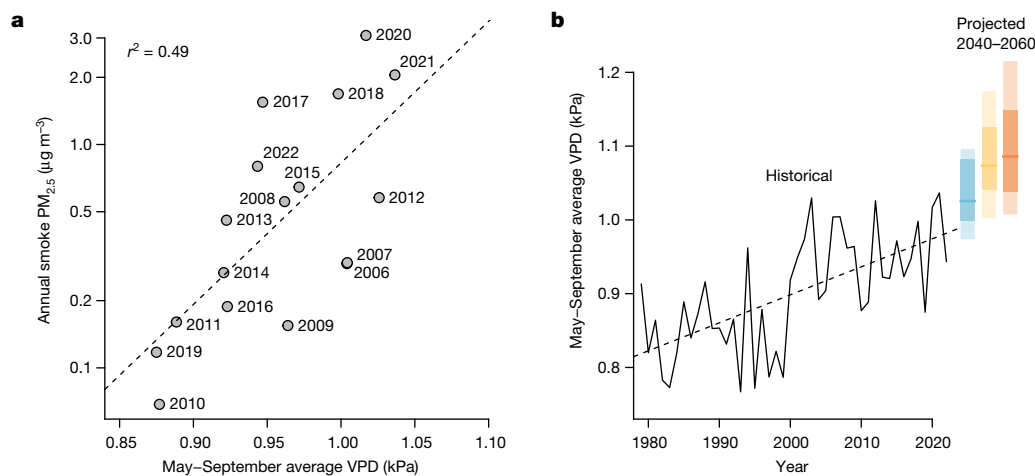


Fig. 4 | Climate is a strong historical driver of interannual variation in smoke exposure, and projected mid-century changes in climatic drivers exceed recent historical extremes. **a**, Interannual variation in summertime (May–September) VPD averaged over western forests is a strong predictor of annual variation in the log of average smoke $PM_{2.5}$ variation across the US West, 2006–2022 ($r^2 = 0.49$); smoke $PM_{2.5}$ is a simple average of daily smoke $PM_{2.5}$ over all reporting stations in the US West in a given year, and the dotted line is linear regression fit. **b**, Historical and projected mid-century changes in summertime VPD over western forests. Rectangles to the right show projected mid-century

(2040–2060) average summertime VPD from an ensemble of 34 GCMs run under the listed emissions scenarios and debiased to match observed VPD values in a common 1979–2014 sample; lighter rectangles are 10th–90th percentiles, darker rectangles are interquartile range and solid horizontal line is ensemble median. Mid-century ensemble median projected values across all emissions scenarios exceed recent multi-year VPD averages and are as large or larger than recent historical extremes, suggesting that smoke $PM_{2.5}$ is likely to continue to increase absent of extra intervention.

Data Fig. 8). Between 2011 and 2022, wildfire smoke caused at least 25% of exceedances in seven states (Washington, Oregon, Montana, Idaho, Nevada, North Dakota and South Dakota). In the the last 3 years of the sample (2020–2022), wildfire smoke caused at least 25% of daily exceedances in 21 states and caused more than 75% of exceedances in four states (Washington, Oregon, Montana and Idaho). We conclude that wildfire smoke has been a substantial cause of increases in daily $PM_{2.5}$ extremes throughout most of the West, and that the influence of smoke on extremes now extends beyond the influence uncovered in previous analyses¹³, which discerned influence only in the Pacific northwest.

Historical and future climatic influence

The recent rapid uptick in wildfire activity and resulting upward pressure on annual and extreme $PM_{2.5}$ concentrations throughout the western USA raises the question of whether recent $PM_{2.5}$ trends are likely to continue or whether they were driven by idiosyncratic variability in climatic conditions that are unlikely to persist. Many studies have sought to understand climatic drivers of recent increases in fire activity and to project future changes in these drivers. Together, these studies provide strong evidence that interannual variation in climate-related factors such as fuel aridity and fire weather are a primary driver of recent variation in fire activity, and that projected future changes in these variables from global climate models (GCMs) indicate that—absent intervention—fire activity is likely to further increase as the climate warms^{7,23}, although the magnitude of that increase is sensitive to the climate variable used to project changes in wildfire activity²⁴. Using a variety of modelling approaches, studies also relate projected increases in wildfire activity to potential changes in surface air quality over the next century, finding large possible increases in average and daily extreme $PM_{2.5}$ concentrations^{25,26}.

To further corroborate these results, we calculate annual summertime (May to September) average vapour pressure deficit (VPD) over western US forests, and relate these values to our measures of annual average smoke $PM_{2.5}$, using all available monitoring stations across the western USA (defined here as all states in the CONUS west of, and including, New Mexico, Colorado, Wyoming and Montana). Summertime VPD is

strongly related to the log of smoke $PM_{2.5}$ (Fig. 4a), explaining half its interannual variation since 2006. The estimated relationship is robust to first detrending both VPD and smoke, and so is not spuriously driven by common time trends in both time series. VPD values have increased over western forests since 1980, and were at or near record maxima in recent years (Fig. 4b).

Using an ensemble of 34 debiased GCM projections (Methods), we find that projected average VPD levels over western forests by mid-century match or exceed recent historical extremes, even under low greenhouse gas emissions scenarios (Fig. 4b). Relative to observed VPD in the last 5 years of our sample (2018–2022), ensemble median projected average increases in VPD under SSP3-7.0 indicate an extra increase in annual average smoke $PM_{2.5}$ concentrations of $3.1 \mu g m^{-3}$ by 2050, on the basis of the log-linear relationship in Fig. 4a. This projected increase represents an annual growth rate in smoke $PM_{2.5}$ in future years (roughly $0.1 \mu g m^{-3} yr^{-1}$) that is nearly equivalent to the annual growth rate observed during the 2016–2022 period in these western states ($0.12 \mu g m^{-3} yr^{-1}$). The ensemble mean projected change in smoke is more than twice these median estimates, a result of the estimated exponential relationship between VPD and smoke $PM_{2.5}$. These results indicate that recent trends in smoke $PM_{2.5}$ will probably continue under a warming climate. However, we warn that such projections assume that future smoke-VPD relationships will mirror past relationships, which might not be the case if widespread wildfires or human fuels management limit future fuel abundance. More detailed dynamic and spatially explicit modelling is critically needed to better understand how smoke will evolve under future climate.

Discussion

Approaches to air quality regulation have historically been built on two primary facts: most pollutant concentrations were the results of emissions tied directly to controllable human activity, and the sources of these emissions tended to be locally or regionally proximate to the population that they affect. Regulation based largely on these facts, such as the Clean Air Act, have contributed substantially to the remarkable decadal improvements in air quality averages and

extremes observed throughout the USA through the early 2010s (ref. 2) (Fig. 1 and Extended Data Fig. 3). These facts have also led to calls for location-specific approaches to reducing remaining pollution burdens and eliminating remaining disparities in exposures across socioeconomic groups²⁷. At present, EPA is in the process of reviewing and revising the level of permitted ambient PM_{2.5} under the Clean Air Act on the basis of updated scientific recommendations of 8–10 µg m⁻³ annual average PM_{2.5} (ref. 28).

We show that recent increases in wildfire smoke have substantially slowed or reversed improvements in ambient PM_{2.5} concentrations throughout much of the USA, with widespread recent influence on annual average PM_{2.5} concentrations and regional influence on daily PM_{2.5} extremes. These increases in wildfire smoke, which we and others show are expected to continue under a warming climate, subvert the logic of traditional, regionally based air quality regulation focused on control of anthropogenic emission sources and could undermine location-specific approaches to reducing pollution burdens. This is because with wildfires, the emissions source is often not under the control of the affected jurisdiction: increased surface pollutant concentrations in one location can originate from fires that are hundreds or thousands of kilometres away²², and these fires have a more indirect—albeit substantial—link to human activity. Whereas more recent US rule making, such as the Cross-State Air Pollution Rule, recognizes that criteria pollutants often cross-state boundaries, such regulation at present only pertains to large power plants in 27 states in the Eastern USA. Further, wildfire smoke remains explicitly exempted from both local and transboundary attainment rules under the Clean Air Act, while, at the same time, proposed approaches to better managing wildfire and wildfire smoke, by means of greater use of prescribed fire, are subject to regulation under the Act because they are considered anthropogenic emissions sources^{29,30}. The growing influence of wildfire smoke on ambient PM_{2.5} trends that we document suggests that a continuation of this current regulatory approach could increasingly fail to protect public health from poor ambient air quality.

New approaches will probably be needed to address the growing influence of wildfire smoke on air quality. These could include large-scale investment in fuels management to reduce extreme wildfire risk, as recently proposed by the US Forest Service²⁹; revision to key air quality regulation such that air quality exemptions during smoke days are only granted if efforts have been made to reduce wildfire risk; a default stance (or ‘rebuttable presumption’) that prescribed fire smoke emissions are exempt from regulation under the Clean Air Act, especially if annual average regulatory PM_{2.5} standards are lowered; and expansion of the geographic scope of regulatory implementation plans to include both source and affected jurisdictions and/or a shift in focus of air pollution programmes towards exposure rather than emission reduction, indicating large investment in indoor filtration to protect individuals and communities from the wildfire smoke events that increasingly occur^{6,17,31}. Given the complexity of wildfire smoke management, all these measures may be required to avoid significant negative effects on public health. Absent of these or other interventions, wildfires’ contribution to poor air quality and adverse health effects will probably continue to grow as the climate continues to warm.

Online content

Any methods, additional references, Nature Portfolio reporting summaries, source data, extended data, supplementary information, acknowledgements, peer review information; details of author contributions and competing interests; and statements of data and code availability are available at <https://doi.org/10.1038/s41586-023-06522-6>.

1. Currie, J. & Walker, R. What do economists have to say about the clean air act 50 years after the establishment of the environmental protection agency? *J. Econ. Perspectives* **33**, 3–26 (2019).

2. Aldy, J. E., Auffhammer, M., Cropper, M., Fraas, A. & Morgenstern, R. Looking back at 50 years of the Clean Air Act. *J. Econ. Lit.* **60**, 179–232 (2022).
3. *Benefits and Costs of the Clean Air Act 1990–2020. Report Documents and Graphics* (US Environmental Protection Agency, 2011); <https://www.epa.gov/clean-air-act-overview/benefits-and-costs-clean-air-act-1990-2020-report-documents-and-graphics>.
4. Correia, A. W. et al. The effect of air pollution control on life expectancy in the United States: an analysis of 545 US counties for the period 2000 to 2007. *Epidemiology* **24**, 23–31 (2013).
5. Clay, K., Muller, N. Z. & Wang, X. Recent increases in air pollution: evidence and implications for mortality. *Rev. Environ. Econ. Policy* **15**, 154–162 (2021).
6. Burke, M. et al. The changing risk and burden of wildfire in the United States. *Proc. Natl Acad. Sci. USA* **118**, e2011048118 (2021).
7. Abatzoglou, J. T. & Williams, A. P. Impact of anthropogenic climate change on wildfire across western US forests. *Proc. Natl Acad. Sci. USA* **113**, 11770–11775 (2016).
8. Parks, S. A. & Abatzoglou, J. T. Warmer and drier fire seasons contribute to increases in area burned at high severity in western US forests from 1985 to 2017. *Geophys. Res. Lett.* **47**, e2020GL089858 (2020).
9. Juang, C. S. et al. Rapid growth of large forest fires drives the exponential response of annual forest-fire area to aridity in the western United States. *Geophys. Res. Lett.* **49**, e2021GL097131 (2022).
10. Boisramé, G. F., Brown, T. J. & Bachelet, D. M. Trends in western USA fire fuels using historical data and modeling. *Fire Ecol.* **18**, 8 (2022).
11. Balch, J. K. et al. Human-started wildfires expand the fire niche across the United States. *Proc. Natl Acad. Sci. USA* **114**, 2946–2951 (2017).
12. Landrigan, P. J. et al. The Lancet commission on pollution and health. *Lancet* **391**, 462–512 (2018).
13. McClure, C. D. & Jaffe, D. A. US particulate matter air quality improves except in wildfire-prone areas. *Proc. Natl Acad. Sci. USA* **115**, 7901–7906 (2018).
14. O’Dell, K., Ford, B., Fischer, E. V. & Pierce, J. R. Contribution of wildland-fire smoke to US PM_{2.5} and its influence on recent trends. *Environ. Sci. Technol.* **53**, 1797–1804 (2019).
15. Xie, Y., Lin, M. & Horowitz, L. W. Summer PM_{2.5} pollution extremes caused by wildfires over the western United States during 2017–2018. *Geophys. Res. Lett.* **47**, e2020GL089429 (2020).
16. Childs, M. L. et al. Daily local-level estimates of ambient wildfire smoke PM_{2.5} for the contiguous US. *Environ. Sci. Technol.* **56**, 13607–13621 (2022).
17. David, L. M. et al. Could the exception become the rule? ‘Uncontrollable’ air pollution events in the US due to wildland fires. *Environ. Res. Lett.* **16**, 034029 (2021).
18. Tschofen, P., Azevedo, I. L. & Muller, N. Z. Fine particulate matter damages and value added in the US economy. *Proc. Natl Acad. Sci. USA* **116**, 19857–19862 (2019).
19. Burney, J. A. The downstream air pollution impacts of the transition from coal to natural gas in the United States. *Nat. Sustain.* **3**, 152–160 (2020).
20. Shapiro, J. S. Pollution trends and US environmental policy: lessons from the past half century. *Rev. Environ. Econ. Policy* **16**, 42–61 (2022).
21. Muggeo, V. M. Estimating regression models with unknown break-points. *Stat. Med.* **22**, 3055–3071 (2003).
22. Brey, S. J., Ruminski, M., Atwood, S. A. & Fischer, E. V. Connecting smoke plumes to sources using hazard mapping system (HMS) smoke and fire location data over North America. *Atmospheric Chem. Phys.* **18**, 1745–1761 (2018).
23. Goss, M. et al. Climate change is increasing the likelihood of extreme autumn wildfire conditions across California. *Environ. Res. Lett.* **15**, 094016 (2020).
24. Brey, S. J., Barnes, E. A., Pierce, J. R., Swann, A. L. & Fischer, E. V. Past variance and future projections of the environmental conditions driving western US summertime wildfire burn area. *Earth’s Future* **9**, e2020EF001645 (2021).
25. Xie, Y. et al. Tripling of western US particulate pollution from wildfires in a warming climate. *Proc. Natl Acad. Sci. USA* **119**, e2111372119 (2022).
26. Neumann, J. E. et al. Estimating PM_{2.5}-related premature mortality and morbidity associated with future wildfire emissions in the western US. *Environ. Res. Lett.* **16**, 035019 (2021).
27. Wang, Y. et al. Location-specific strategies for eliminating US national racial-ethnic PM_{2.5} exposure inequality. *Proc. Natl Acad. Sci. USA* **119**, e2205548119 (2022).
28. *Policy Assessment for the Reconsideration of the National Ambient Air Quality Standards for Particulate Matter* (US Environmental Protection Agency, 2022); https://www.epa.gov/system/files/documents/2022-05/Final%20Policy%20Assessment%20for%20the%20Reconsideration%20of%20the%20PM%20NAAQS_May2022_0.pdf.
29. *Confronting the Wildfire Crisis: A Strategy for Protecting Communities and Improving Resilience in America’s Forests, FS-1187a* (US Forest Service, 2022); https://www.fs.usda.gov/sites/default/files/fs_media/fs_document/Confronting-the-Wildfire-Crisis.pdf.
30. *Exceptional Events Guidance: Prescribed Fire on Wildland that May Influence Ozone and Particulate Matter Concentrations* (US Environmental Protection Agency, 2019); https://www.epa.gov/sites/default/files/2019-08/documents/ee_prescribed_fire_final_guidance_-_august_2019.pdf.
31. Williams, E. Reimagining exceptional events: regulating wildfires through the Clean Air Act. *Wash. L. Rev.* **96**, 765 (2021).
32. *Particulate Matter (PM_{2.5}) Trends* (US Environmental Protection Agency, 2022); <https://www.epa.gov/air-trends/particulate-matter-pm25-trends>.
33. Karl, T. & Koss, W. J. *Regional and National Monthly, Seasonal, and Annual Temperature Weighted by Area, 1895–1983*. NOAA Climatology History Series 4-3 (NOAA, 1984).

Publisher’s note Springer Nature remains neutral with regard to jurisdictional claims in published maps and institutional affiliations.

Springer Nature or its licensor (e.g. a society or other partner) holds exclusive rights to this article under a publishing agreement with the author(s) or other rightsholder(s); author self-archiving of the accepted manuscript version of this article is solely governed by the terms of such publishing agreement and applicable law.

© The Author(s), under exclusive licence to Springer Nature Limited 2023

Methods

Isolating wildfire smoke $PM_{2.5}$

We measure total $PM_{2.5}$ at the daily level using data from 2,498 EPA air quality monitoring stations located throughout the CONUS, where station-day average $PM_{2.5}$ is calculated over all observations from monitors at a station location (Extended Data Fig. 1)^{34,35}. To understand when smoke from fires may be affecting ground pollution levels, we follow earlier work^{14,16,36} and construct a binary classification of smoke days for each station-day using data on smoke plumes from the National Oceanic and Atmospheric Administration hazard mapping system (HMS)³⁷, which are analyst-identified plume boundaries based on visible bands of satellite imagery^{38–40}. A station-day is classified as a smoke day if it falls within a smoke plume on a given day. The first full year for which the HMS plume data are available is 2006, which limits the start date of our smoke estimates.

We then combine ground station measurements with this classification of smoke days to define daily time series of smoke $PM_{2.5}$ at each station. We first define $PM_{2.5}$ anomalies as deviations from recent month- and location-specific median values on non-smoke days

$$\overline{PM}_{idmy} = PM_{idmy} - \overline{PM}_{imY}^{NS}, \quad (1)$$

where PM_{idmy} is the $PM_{2.5}$ at station i on day d in month m and year y , and \overline{PM}_{imY}^{NS} is the 3-year location- and month-specific median $PM_{2.5}$ on non-smoke (NS) days. This median is calculated as

$$\overline{PM}_{imY}^{NS} = \text{median}(\{PM_{idmy} | i = I, m = M, Y - 1 \leq y \leq Y + 1, \text{smoke}_{idmy} = 0\}), \quad (2)$$

with smoke_{idmy} a binary variable indicating smoke-day classification, or when smoke may be affecting air pollution levels. We use medians rather than means to prevent days with extreme $PM_{2.5}$ that are not smoke days from affecting the background $PM_{2.5}$ estimates, as is occasionally the case in our data. Further, by using 3-year medians, we allow the measure of background non-smoke $PM_{2.5}$ to evolve over time in each location to capture trends in non-smoke $PM_{2.5}$, which include the many other changing sources of anthropogenic emissions. We then define smoke $PM_{2.5}$ on each station-day as the anomaly relative to the median if there was a plume overhead; this allows negative smoke values on days when total $PM_{2.5}$ was below median $PM_{2.5}$ on a day with a plume overhead, which in our data occur on 2.36% of all station-days. We also tested robustness to bottom-coding smoke at zero, that is, setting negative values of smoke $PM_{2.5}$ to zero, and find that this yields higher classifications of smoke influence (Extended Data Table 2). Finally, we calculate non-smoke $PM_{2.5}$ on each station-day as the difference between total $PM_{2.5}$ on that day and estimated smoke $PM_{2.5}$ on that day.

Our approach to isolating smoke $PM_{2.5}$ at monitoring stations is similar to other recent work^{14,16,36}, and for it to successfully isolate wildfire's contribution to surface $PM_{2.5}$, it must be the case that the HMS plumes accurately describe the location of wildfire smoke on a given day and that the presence or absence of a plume is not correlated with other non-wildfire sources of variation in surface $PM_{2.5}$. To the first concern, we find in our data that having a smoke plume overhead is associated with an average $4.67 \mu\text{g m}^{-3}$ increase in $PM_{2.5}$ after controlling for station-specific averages and average differences in $PM_{2.5}$ between states, months and years using fixed-effects regression. We also find that in time series for specific stations, plumes align temporally with spikes in ground-measured $PM_{2.5}$ (Extended Data Fig. 1). We note that our approach does not require that plume heights or plume density be accurately measured by the satellite data; rather, we only need the plume data to tell us whether there is any smoke in the atmospheric column, and then the magnitude of the ground-measured $PM_{2.5}$ anomaly under the plume will tell us whether this smoke is mixing to the surface and how much it is affecting surface pollutant concentrations.

To the second concern about correlated time-varying non-smoke $PM_{2.5}$ sources, Childs et al.¹⁶ analysed whether this method of constructing smoke $PM_{2.5}$ from ground station anomalies is indeed picking up $PM_{2.5}$ from smoke and not from other local time-varying sources of $PM_{2.5}$ unrelated to smoke by using speciated data from Interagency Monitoring of Protected Visual Environments (IMPROVE) and Chemical Speciation Network monitors. The authors found that species most likely to be present in smoke $PM_{2.5}$ —in particular organic carbon—rose on smoke days but other non-fire-associated species (for example, elemental carbon) did not rise. These results provide supporting evidence that our approach to isolating smoke $PM_{2.5}$ from non-smoke $PM_{2.5}$ is indeed picking up wildfire-sourced $PM_{2.5}$ and not some other correlated $PM_{2.5}$ source. Nevertheless, our measure of smoke days may still be a conservative estimate of the locations with air quality affected by smoke: there probably remain undetected plumes under cloud cover, during nighttime periods when satellite-based plume segmentations are unavailable or on days when smoke is diffuse and difficult to identify in satellite imagery^{14,22}. This will cause us to under-attribute $PM_{2.5}$ to smoke and thus understate the influence of wildfire smoke on total $PM_{2.5}$.

Our main analysis uses data from all EPA monitors between January 2000 and December 2022. Because we use data from fixed pollution stations to measure overall $PM_{2.5}$ trends and wildfire influence on them, our data will be representative of locations where stations are located. As stations are purposefully located in populated areas to assess Clean Air Act attainment, our estimates should be largely representative of CONUS populations. However, they will be less accurate for many rural areas in the western USA where stations are less common but in which other estimates suggest wildfire influence on $PM_{2.5}$ is often the strongest¹⁶. Our implicitly population-weighted estimates thus probably understate the influence of smoke on total $PM_{2.5}$ trends relative to an area-weighted estimate, and could understate wildfire influence in the rural West.

Finally, our approach to estimating trends in total, smoke and non-smoke $PM_{2.5}$ that combines satellites and ground stations is a complement to other potential approaches to measuring the influence of smoke on air quality trends, including approaches that rely on statistical analysis of station data alone¹³ or that use emissions inventories and chemical transport models^{14,15}. An advantage of our approach relative to solely station-based approaches is that satellite-derived plume data provide substantial information on the location of wildfire smoke plumes, and this information helps isolate the influence of wildfires from other time-trending sources of pollution exposure. An advantage of our approach relative to transport-based approaches is that it does not depend on uncertain wildfire emissions inventories, which have been shown to have large influence on predicted pollutant concentrations⁴¹. Machine-learning based approaches for total and wildfire $PM_{2.5}$, and the gridded products they generate, provide an alternate approach^{16,42,43}, yet these products are generally estimated with some time lag and do not yet provide estimates for the most recent, heavy wildfire smoke years.

Estimating trend breaks and period-specific trends

To split our data into early and recent periods, estimate trends in total and non-smoke $PM_{2.5}$ in each period, and test whether slopes differ across periods or pollutants, we use the following bootstrap procedure. First, we restrict our sample to all available stations in CONUS that meet an inclusion criteria, which in our main sample is having more than 50 daily observations per year for at least 15 years (we test robustness to this criteria as described below). We draw a stratified random sample of stations from this dataset, stratifying on state and sampling with replacement. We use state-stratified random sampling to ensure that each state has the same influence on the pooled estimate in each bootstrap, and sampling monitoring stations with replacement mimics the idea of an (unobserved) superpopulation of possible pollution monitor locations in each state, of which we observe only a sample.

Using this sample, we then follow ref. 21 and implement an algorithmic approach to estimating breakpoints in time series data. Under this approach, a breakpoint initialization value is chosen and the algorithm searches until the change in the estimated breakpoint falls within a prespecified tolerance level. Formally, we search for a single breakpoint ψ^* by fitting the following iterative regression on the station-year data:

$$y_{it} = \alpha_i + \delta_1 z_t + \delta_2 (z_t - \tilde{\psi}) \mathbb{1}\{z_t > \tilde{\psi}\} - \gamma \mathbb{1}\{z_t > \tilde{\psi}\} + \varepsilon_{it} \quad (3)$$

where y is total $\text{PM}_{2.5}$ at station i in year t , α_i is a vector of station fixed effects (intercepts), z_t is a numeric variable indexing time, $\tilde{\psi}$ is the iteratively updated candidate breakpoint, γ measures the gap at a given iteration of breakpoint $\tilde{\psi}$ between the two fitted lines on either side of the breakpoint and $\mathbb{1}\{z_t > \tilde{\psi}\}$ is the indicator function, and δ_1 and δ_2 are estimated period-specific time trends. The breakpoint is then updated between iterations, with $\tilde{\psi} = \tilde{\psi} + \frac{\gamma}{\delta_2}$. As the algorithm converges, the ratio $\frac{\gamma}{\delta_2}$ approaches zero, with the algorithm ceasing once it falls within a prespecified tolerance, which we set to 1×10^{-8} (see Supplemental Methods for a discussion of robustness to weaker and stronger tolerances). We also constrain the algorithm to search only between the 20th and 80th quantile of the time series for CONUS breakpoints and between the 15th and 85th quantile for regional breakpoints, preventing it from choosing breakpoints in the first or last few years of the sample. This was done to prevent the pre- and postperiod model fits from having to use only a very small slice of the sample, which could lead to very steep, imprecisely estimated slopes that are both noisy and a poor predictor of future trends. The model sees only total $\text{PM}_{2.5}$ data when estimating the breakpoint. Less strict quantile constraints were chosen for the regional breakpoints to account for variation in possible breaks across regions. See Supplemental Methods for further details on algorithm implementation.

Once a breakpoint is chosen on the pooled data, we then fit generalized linear maximum likelihood panel regressions⁴⁴ to the same sample of station-year observations, pooling stations within a given region of interest (typically, state) and allowing slopes to differ on either side of the prescribed breakpoint. Formally, we estimate equations of the following form separately for both total and non-smoke $\text{PM}_{2.5}$:

$$\text{PM}_{its} = \alpha_{is} + \beta_{1s} (z_t - \psi^*) \mathbb{1}\{z_t \leq \psi^*\} + \beta_{2s} (z_t - \psi^*) \mathbb{1}\{z_t > \psi^*\} + \varepsilon_{its} \quad (4)$$

where ψ^* is the estimate of the breakpoint generated from the algorithm described above. The subscript i indexes pollution station, t is the year and s is the type of particulate matter (total or non-smoke $\text{PM}_{2.5}$). $\mathbb{1}\{\}$ is the indicator function, α_{is} represents a station- $\text{PM}_{2.5}$ type intercept (that is, separate intercepts for each station and $\text{PM}_{2.5}$ type of total or non-smoke) and β_{1s} and β_{2s} are the estimates of early and recent-period slopes for $\text{PM}_{2.5}$ type s , pooled across all stations i . This equation is estimated either using all stations in CONUS, or all stations in a given state or region, yielding a set of estimates of state- and period-specific trends in total and non-smoke $\text{PM}_{2.5}$.

We construct 1,000 stratified bootstrap samples, then repeat this entire procedure for each bootstrap, generating 1,000 breakpoint estimates and 1,000 estimates of the slopes for each state and for CONUS. The distribution of these estimates (Extended Data Fig. 2) thus accounts for uncertainty in both the timing of the breakpoint as well as uncertainty in the slopes conditional on a chosen breakpoint. The analysis is repeated separately for annual average $\text{PM}_{2.5}$ and for the proportion of days in which $\text{PM}_{2.5}$ is greater than $35 \mu\text{g m}^{-3}$ as outcomes. For annual average $\text{PM}_{2.5}$, our maximum likelihood estimator is equivalent to estimating equation (4) with ordinary least squares; for annual counts of extreme days, we instead use a Poisson fixed-effects model to find the breakpoint and fit slopes, with counts of extreme days per year as the outcome and log of number of station-year observations as an offset.

We then use these bootstrapped distributions of slope estimates to implement statistical tests: whether early-period (β_1) and recent-period

(β_2) slopes in total $\text{PM}_{2.5}$ are statistically different and whether the recent-period slope (β_2) is different from zero, to classify states as stagnating, reversing, accelerating or not significantly changing; and whether slopes in recent-period total $\text{PM}_{2.5}$ (β_2) and non-smoke $\text{PM}_{2.5}$ (β'_2) are different, to classify smoke influence. Differences are classified as statistically significant if 97.5% of the distribution of differences in slopes (for example, $\beta_1 - \beta_2$) is on one side of zero, that is, $P < 0.05$ on a two-tailed test. Details on classifications are provided in Extended Data Table 1.

We test robustness in various ways: to alternate station inclusion criteria, to the inclusion or exclusion of recent very-high-wildfire years and to the use of regional rather than national breakpoints, using the nine climate regions in Fig. 1 to define the regions within which separate breakpoints are estimated. As shown in Extended Data Figs. 5–7 and Extended Data Table 2, results are largely robust to these choices. A few factors contribute to the observed variation in results. First, stricter station inclusion criteria drive down sample size and thus tend to decrease power and spatial representativeness. Second, some inclusion criteria yield bootstrap samples with higher variance in the distribution of estimated breakpoints. Samples with a higher percentage of earlier breakpoints will tend to estimate more similar pre- and postbreak slopes, resulting in more stagnation and fewer reversal classifications. Third, removal of 2021 has the most influence on estimates, and removing it from the analysis results in 17 fewer states classified as smoke influenced for average annual $\text{PM}_{2.5}$ and seven fewer states classified as smoke influenced for portion of days in which $\text{PM}_{2.5}$ is greater than $35 \mu\text{g m}^{-3}$ (Extended Data Table 2 and Extended Data Fig. 7). Given that VPD over western forests is a strong driver of wildfire smoke, that 2021 was a year of historically high VPD over western forests and that future VPD averages are likely to exceed these historical extremes (Fig. 4), inclusion of 2021 in the sample is arguably important for understanding recent trends in wildfire smoke. Nevertheless, sensitivity of estimates to its exclusion suggests the need to further assess wildfire smoke's contribution in coming years.

We also study how results change if, instead of fitting the continuous model in equation (4) that forces fitted lines to intersect at the breakpoint, we fit a model that allows period-specific intercepts, which does not force intersection at the breakpoint. Whereas such a model is perhaps less sensible for estimating whether trends in total $\text{PM}_{2.5}$ changed between early and recent periods, it is arguably more sensible for estimating whether recent-period total versus non-smoke $\text{PM}_{2.5}$ trends are different; a researcher interested in only the latter question might sensibly start by restricting the sample to the years of interest to estimate the trends (for example, dropping years before 2016), which is equivalent to allowing period-specific intercepts. Under this discontinuous model, results are stronger, with 39 states classified as smoke influenced (Extended Data Table 2).

Finally, we calculate the percent of previous air quality improvements that were undone by recent smoke increase by dividing the estimated increase in smoke $\text{PM}_{2.5}$ in the recent period by the estimated decrease in total $\text{PM}_{2.5}$ in the early period. We bottom-code this value at zero for the small number of states where total $\text{PM}_{2.5}$ was not improving during the early period, and top-code at 100% for the small number of states where recent smoke $\text{PM}_{2.5}$ increases exceeded early-period total $\text{PM}_{2.5}$ increases. We calculate the mean or median percentage reversal across all smoke-influenced CONUS states in each bootstrap, then compute confidence intervals using the distribution of estimates across the 1,000 bootstraps.

Climatic drivers of smoke

Building on earlier work⁷, we calculate the annual average VPD during the warm season (May–September) over forests in western states (as defined above) and relate summertime VPD to the log of annual average smoke $\text{PM}_{2.5}$ as measured across monitoring stations in the same states using linear regression, that is:

$$\log(\text{smokePM}_{2.5,t}) = \alpha + \beta \text{VPD}_t + \varepsilon_t \quad (5)$$

Estimates of β are nearly identical whether the equation is estimated with an extra time trend ($\hat{\beta} = 14.3$, standard error (s.e.) = 2.7) or without one ($\hat{\beta} = 14.6$, s.e. = 3.9); in the former case, the impact of VPD on smoke is estimated using deviations in smoke about a time trend on deviations in VPD, thus accounting for any other variable that is trending over time and correlated with both VPD trends and smoke trends. We chose VPD as the main climatic variable because it is frequently used as a primary fire weather index in previous research, is simple to calculate from temperature and relative humidity, and is highly correlated with other fire weather and dryness measures^{7,45,46}. We calculate average seasonal VPD from daily 4 km-resolution surface temperature and relative humidity over the western USA from GRIDMET⁴⁷. We chose to directly calculate VPD from relative humidity and surface temperature (instead of using VPD archived in GRIDMET) to be consistent with the VPD values calculated for future climate projections (as detailed below). The average VPD over the western USA is then calculated as the weighted average of VPD for each grid cell, weighted by the forest coverage percentage of each grid cell. VPD calculation is performed with the R package bigleaf.

To quantify future change in VPD, we use the projected temperature and relative humidity from the Coupled Model Intercomparison Project Phase 6 GCM ensemble, run under different emissions scenarios. Similar to the historical analysis, we first calculate monthly VPD values for each climate model grid cell falling over western US forests and then calculate the annual average VPD over western USA during May to September for a given model and emissions scenario. We evaluate the changes in VPD across three commonly used climate scenarios constructed as pairs between the shared socioeconomic pathways (SSPs) and the representative concentration pathways: SSP1-2.6, SSP2-4.5 and SSP3-7.0. Consistent with the latest Intergovernmental Panel on Climate Change report and recommendations from ref. 48, we use SSP3-7.0 as the baseline high emission scenario and SSP2-4.5 and SSP1-2.6 as the medium and low emission scenarios. In total, we use projections from 34 GCMs with available temperature and relative humidity at the monthly level for the historical and three climate scenarios.

To remove potential level bias from each GCM, simulated VPD values are debiased on the basis of the calculated difference between the simulated values in the historical simulations and the observational VPD values (1979–2014) for each GCM. To reduce the uncertainty and account for internal variability, we summarize mid-century VPD changes as the average VPD values between 2040 and 2060 for each GCM and emissions scenario. We select one ensemble variant for each of the 34 models, using the first ensemble variant of each model (r1i1p1f1) when possible and use the other ensemble variants if r1i1p1f1 is not available.

To estimate potential changes in future smoke $\text{PM}_{2.5}$ under increasing VPD, we combine estimates from the log-linear model in equation 5 with recent (2020–2022) or mid-century VPD averages. Predicted smoke $\text{PM}_{2.5}$ is calculated as:

$$\overline{\text{smokePM}_{2.5}} = \hat{\alpha}_0 e^{\hat{\alpha} + \hat{\beta} \text{VPD}_s} \quad (6)$$

where $\hat{\alpha}_0$ is the ‘smearing estimate’ $\hat{\alpha}_0 = \sum_{i=1}^n e^{\hat{\varepsilon}_i} / n$ that can accommodate non-normally distributed errors⁴⁹, and s indexes warming scenario. Predictions for future annual average smoke $\text{PM}_{2.5}$ under SSP1-2.6, SSP2-4.5 and SSP3-7.0 scenarios are 1.6, 3.2 and 3.8 $\mu\text{g m}^{-3}$ for the western USA, compared to 0.74 for average VPD over the last 5 years (2018–2022). Thus in the highest warming scenario, this simple model predicts an increase in annual average $\text{PM}_{2.5}$ from smoke of 3.1 $\mu\text{g m}^{-3}$ by mid-century, relative to an average across the last five (historically extreme) years. Owing to the exponential relationship between smoke

$\text{PM}_{2.5}$ and VPD, the predicted mean change in smoke across the climate model ensemble is more than twice the median for each emissions scenario. More detailed work is needed to understand whether such changes are plausible.

Data availability

Data to reproduce all results in the paper are available at <https://github.com/echolab-stanford/wildfire-influence>.

Code availability

Code to reproduce all results in the paper are available at <https://github.com/echolab-stanford/wildfire-influence>.

34. *Outdoor Air Quality Data* (US Environmental Protection Agency, 2023); <https://www.epa.gov/outdoor-air-quality-data/download-daily-data>.
35. *What Does the POC Number Refer To?* (US Environmental Protection Agency, accessed September 2023); <https://www.epa.gov/outdoor-air-quality-data/what-does-poc-number-refer>.
36. Burke, M. et al. Exposures and behavioral responses to wildfire smoke. *Nat. Hum. Behav.* **6**, 1351–1361 (2022).
37. *Hazard Mapping System Fire and Smoke Product* (National Oceanic and Atmospheric Administration, accessed September 2023); <https://www.ospo.noaa.gov/Products/land/hms.html#about>.
38. Schroeder, W. et al. Validation analyses of an operational fire monitoring product: the hazard mapping system. *Int. J. Remote Sens.* **29**, 6059–6066 (2008).
39. Rolph, G. D. et al. Description and verification of the NOAA smoke forecasting system: the 2007 fire season. *Weather. Forecast.* **24**, 361–378 (2009).
40. Ruminski, M., Kondragunta, S., Draxler, R. & Zeng, J. Recent changes to the hazard mapping system. In *Proc. 15th International Emission Inventory Conference* Vol. 15 (EPA, 2006).
41. Koplitz, S. N., Nolte, C. G., Pouliot, G. A., Vukovich, J. M. & Beidler, J. Influence of uncertainties in burned area estimates on modeled wildland fire $\text{PM}_{2.5}$ and ozone pollution in the contiguous US. *Atmos. Environ.* **191**, 328–339 (2018).
42. Di, Q. et al. An ensemble-based model of $\text{PM}_{2.5}$ concentration across the contiguous United States with high spatiotemporal resolution. *Environ. Int.* **130**, 104909 (2019).
43. Reid, C. E., Considine, E. M., Maestas, M. M. & Li, G. Daily $\text{PM}_{2.5}$ concentration estimates by county, zip code, and census tract in 11 western states 2008–2018. *Sci. Data* **8**, 112 (2021).
44. Bergé, L. Efficient estimation of maximum likelihood models with multiple fixed-effects: the R package FENmlm. *DEM Discussion Paper Series* (Department of Economics, Univ. Luxembourg, 2018).
45. Zhuang, Y., Fu, R., Santer, B. D., Dickinson, R. E. & Hall, A. Quantifying contributions of natural variability and anthropogenic forcings on increased fire weather risk over the western United States. *Proc. Natl. Acad. Sci. USA* **118**, e2111875118 (2021).
46. Jain, P., Castellanos-Acuna, D., Coogan, S. C., Abatzoglou, J. T. & Flannigan, M. D. Observed increases in extreme fire weather driven by atmospheric humidity and temperature. *Nat. Clim. Chang.* **12**, 63–70 (2022).
47. Abatzoglou, J. T. Development of gridded surface meteorological data for ecological applications and modelling. *Int. J. Climatol.* **33**, 121–131 (2013).
48. Hausfather, Z. & Peters, G. P. Emissions—the ‘business as usual’ story is misleading. *Nature* **577**, 618–620 (2020).
49. Wooldridge, J. M. *Introductory Econometrics: A Modern Approach* (Cengage Learning, 2015).

Acknowledgements We thank members of Stanford ECHOLab and seminar participants at University of California Berkeley, Columbia, Duke, Montana State, Minnesota and University of California Santa Barbara for helpful comments. Some of the computing for this project was performed on the Sherlock cluster, and we thank Stanford University and the Stanford Research Computing Center for providing computational resources and support that contributed to these research results. M.L.C. was supported by an Environmental Fellowship at the Harvard University Center for the Environment. M.Q. was supported by a fellowship at Stanford’s Center for Innovation in Global Health.

Author contributions M.B. and M.L.C. conceived the project. M.B., M.L.C., B.d.L.C., M.Q. and J.L. analysed data. All authors interpreted results and wrote the paper.

Competing interests The authors declare no competing interests.

Additional information

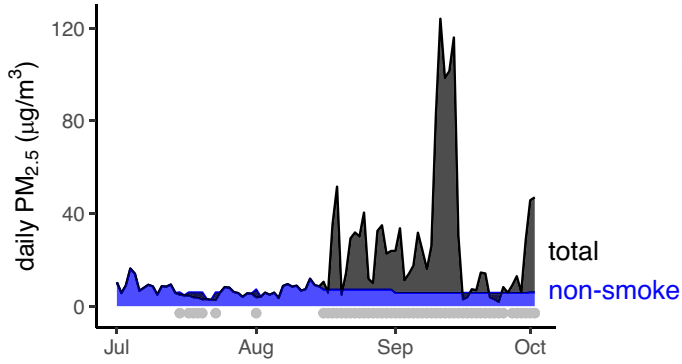
Supplementary information The online version contains supplementary material available at <https://doi.org/10.1038/s41586-023-06522-6>.

Correspondence and requests for materials should be addressed to Marshall Burke.

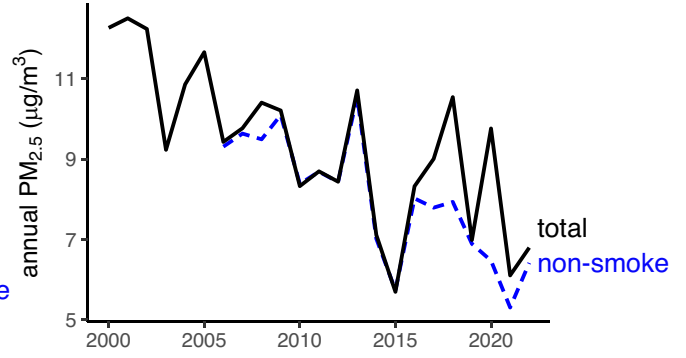
Peer review information Nature thanks Vito Muggego and the other, anonymous, reviewer(s) for their contribution to the peer review of this work. Peer reviewer reports are available.

Reprints and permissions information is available at <http://www.nature.com/reprints>.

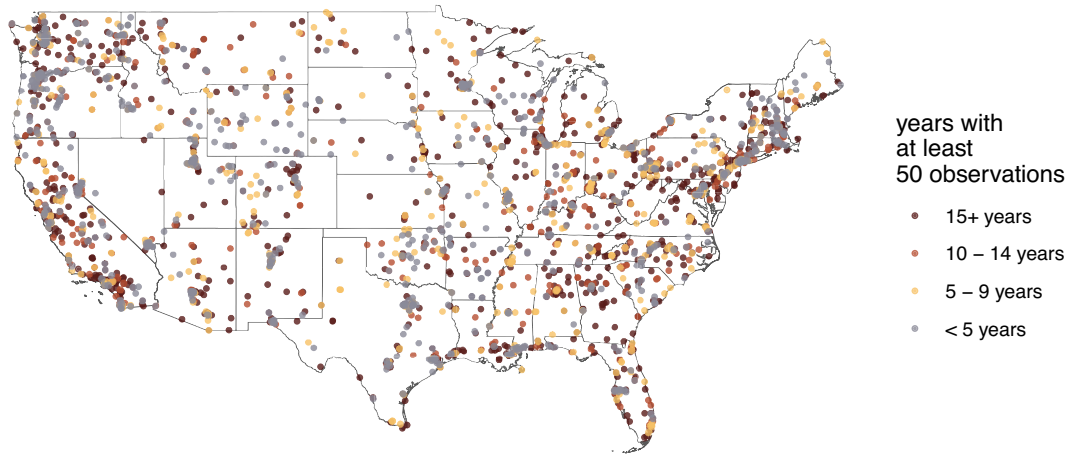
a) Partitioning of total and non-smoke $PM_{2.5}$



b) Annual average by station and year



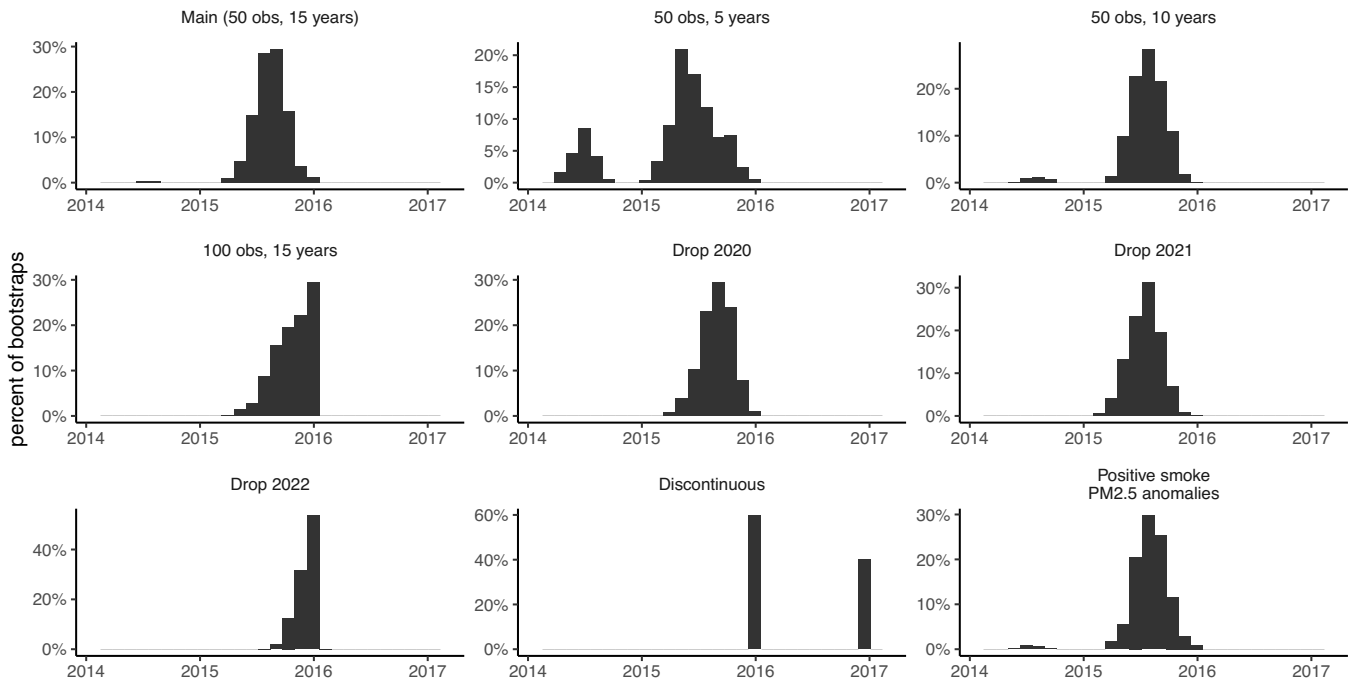
c) Monitor locations and time series lengths



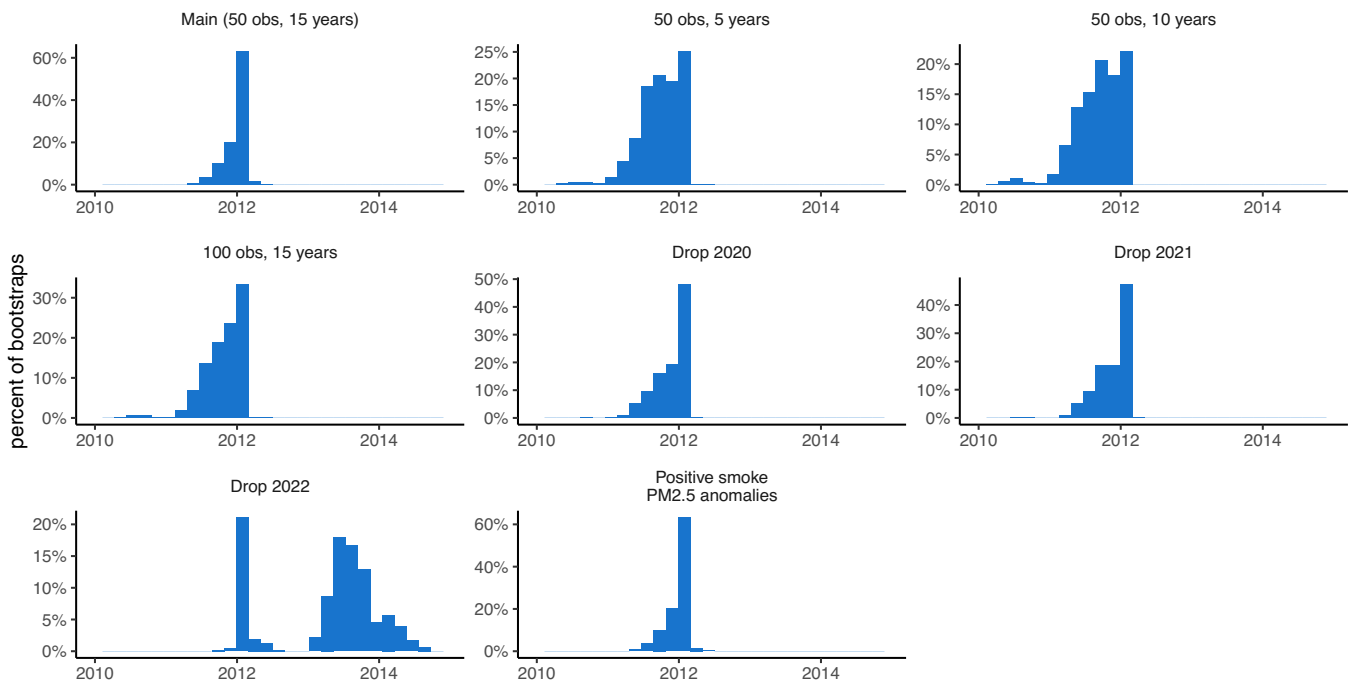
Extended Data Fig. 1 | Pollution stations and method used to construct non-smoke $PM_{2.5}$ estimates. **a.** Example of total and non-smoke partitioning for a single station in CA in 2020. On days without a smoke plume overhead (no grey points), all $PM_{2.5}$ is assumed to be from non-smoke sources. On days with a plume overhead (grey points), $PM_{2.5}$ anomalies from the non-smoke month- and station-specific 3-year median are attributed to smoke, and total

$PM_{2.5}$ minus anomalies are attributed to non-smoke (blue). **b.** Annual average total and non-smoke $PM_{2.5}$ for the same station are produced by aggregating daily total observed $PM_{2.5}$ (black) and the daily estimates of non-smoke $PM_{2.5}$ (blue). **c.** Locations of $PM_{2.5}$ stations throughout the contiguous US. Stations are coloured by the number of years with at least 50 observations.

a. Average annual PM_{2.5}

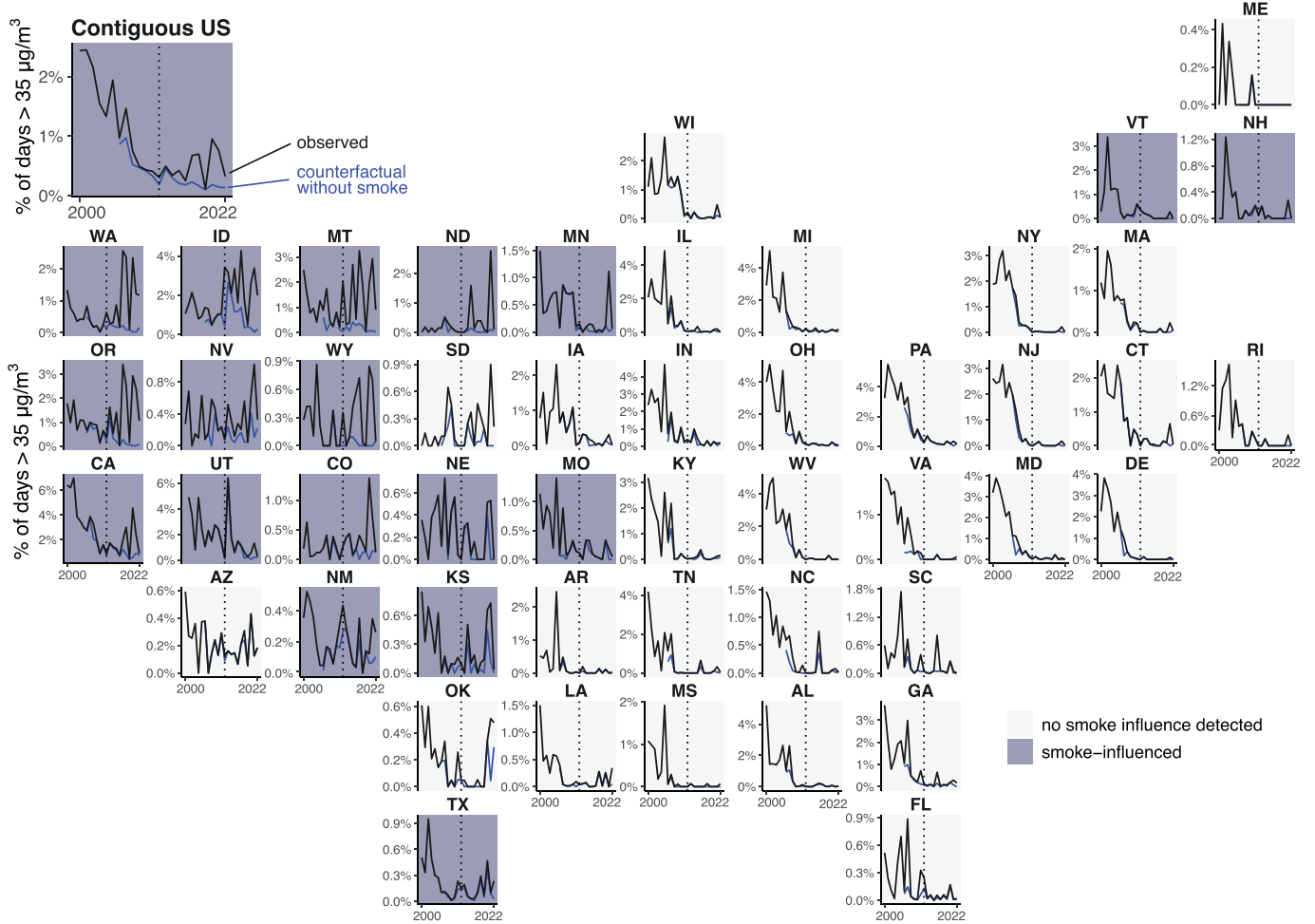


b. Days with extreme PM_{2.5}



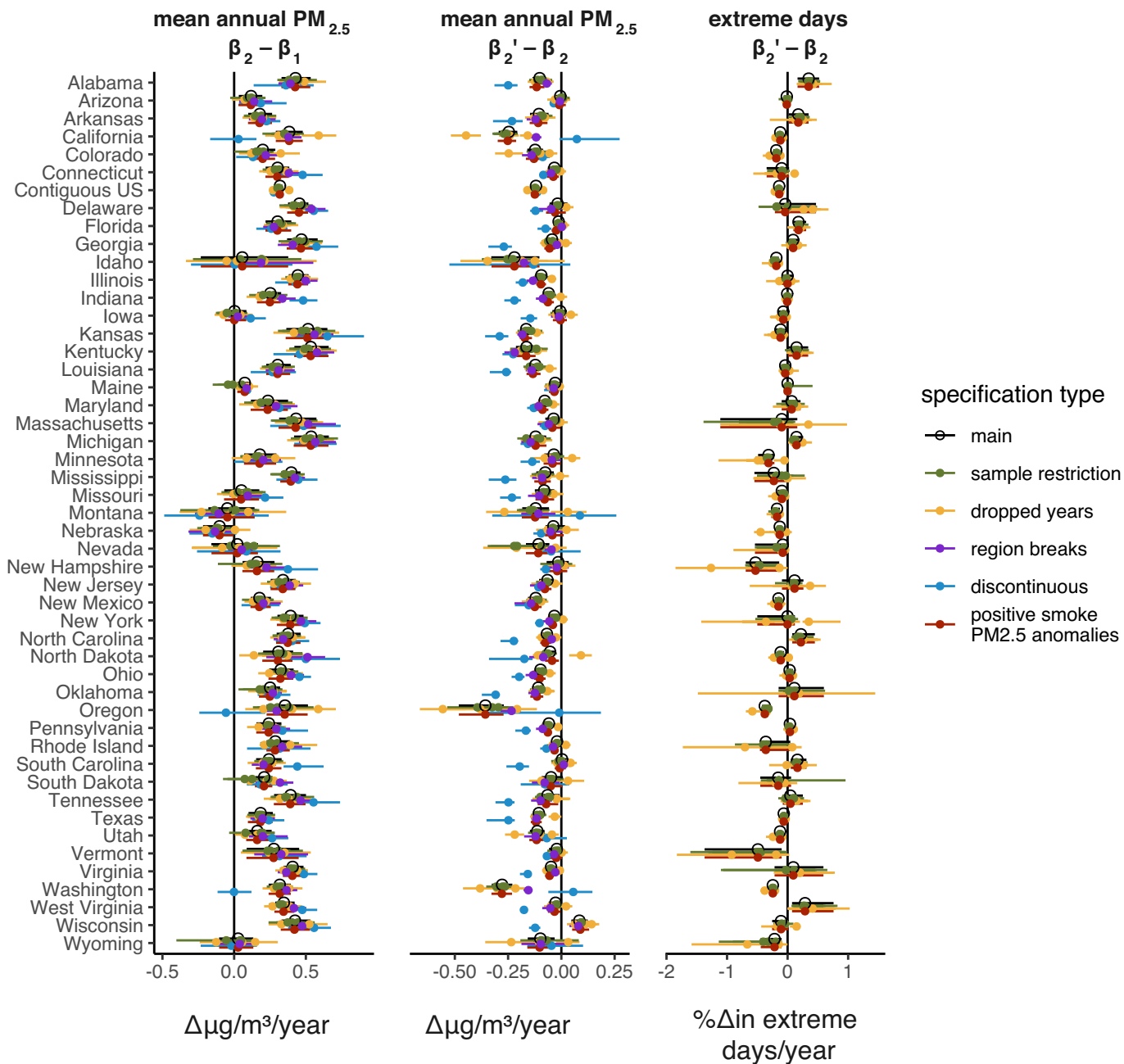
Extended Data Fig. 2 | Distribution in estimated breakpoints for different sample restrictions and/or statistical specifications. a. Annual average PM_{2.5}. **b.** Extreme (> 35 μg/m³) daily PM_{2.5}. Histograms show distribution of estimated breakpoints for different sample restrictions, pooling data from all CONUS monitors. Panels labeled with number of observations and years are various sample restriction choices, while those labeled “Drop” retain our primary inclusion criteria – more than 50 observations per year for at least 15

years – but remove one of the last three years of the sample to understand their influence on estimates. Discontinuous models allow for separate intercepts on either side of the break year. Strong bunching in the discontinuous models for average PM_{2.5} occur because only integer years are permitted as candidate breakpoints. “Positive smoke PM_{2.5} anomalies” tests the sensitivity of results to bottom-coding daily smoke PM_{2.5} estimates to zero, i.e., not allowing negative smoke PM_{2.5} anomalies.



Extended Data Fig. 3 | Influence of wildfire smoke on daily $PM_{2.5}$ extremes is mainly concentrated in states in the West, Northwest, and Great Plains. Black lines in each plot show percent of days in each state-year where $PM_{2.5}$ values exceed $35 \mu g/m^3$, calculated using the sample of stations with over 50

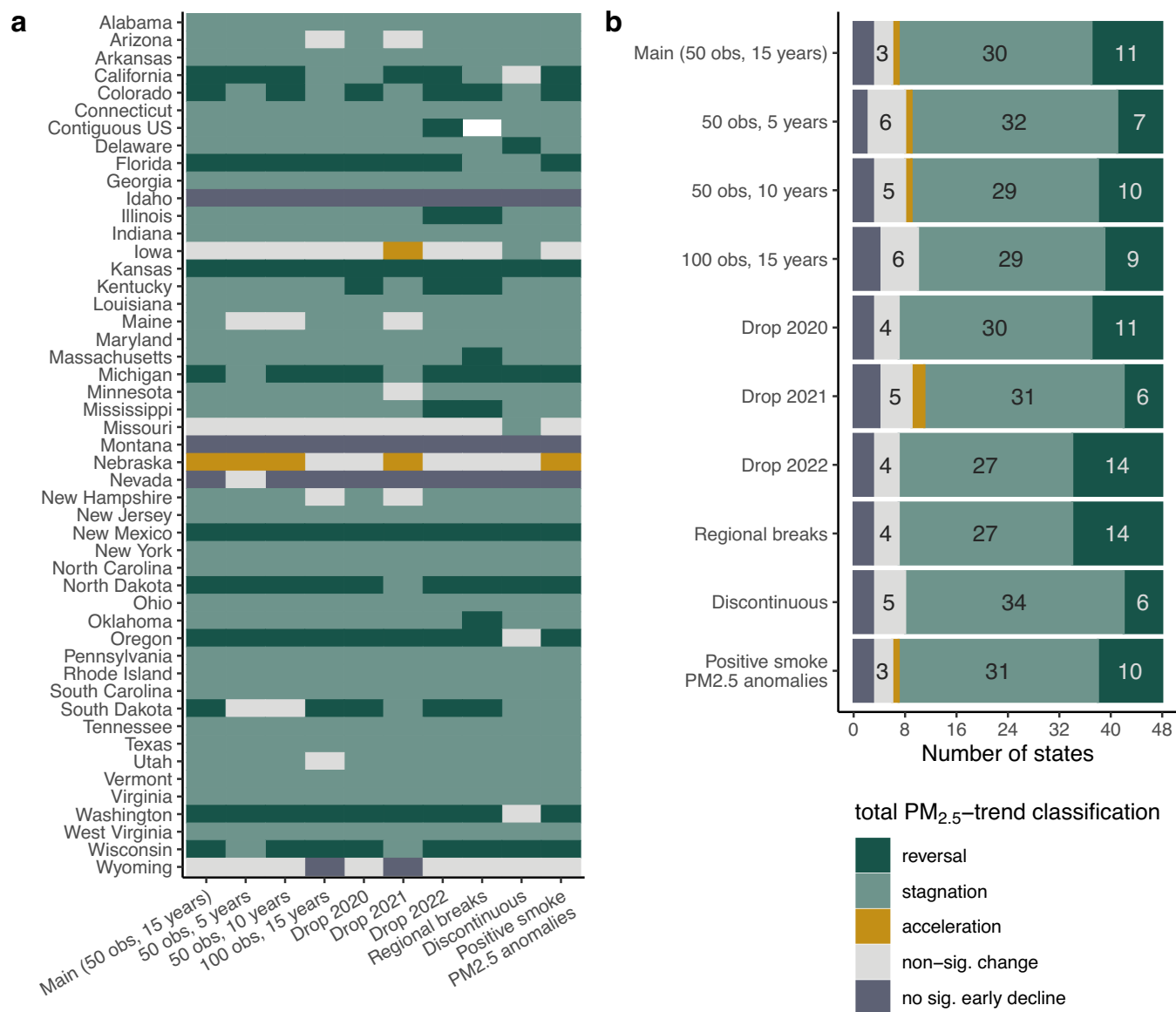
observations in at least 15 years, as in Fig. 3. Blue lines show estimated percent of days that exceed $35 \mu g/m^3$ after smoke $PM_{2.5}$ has been removed. Vertical dotted line indicates median CONUS-wide estimated breakpoint (2012).



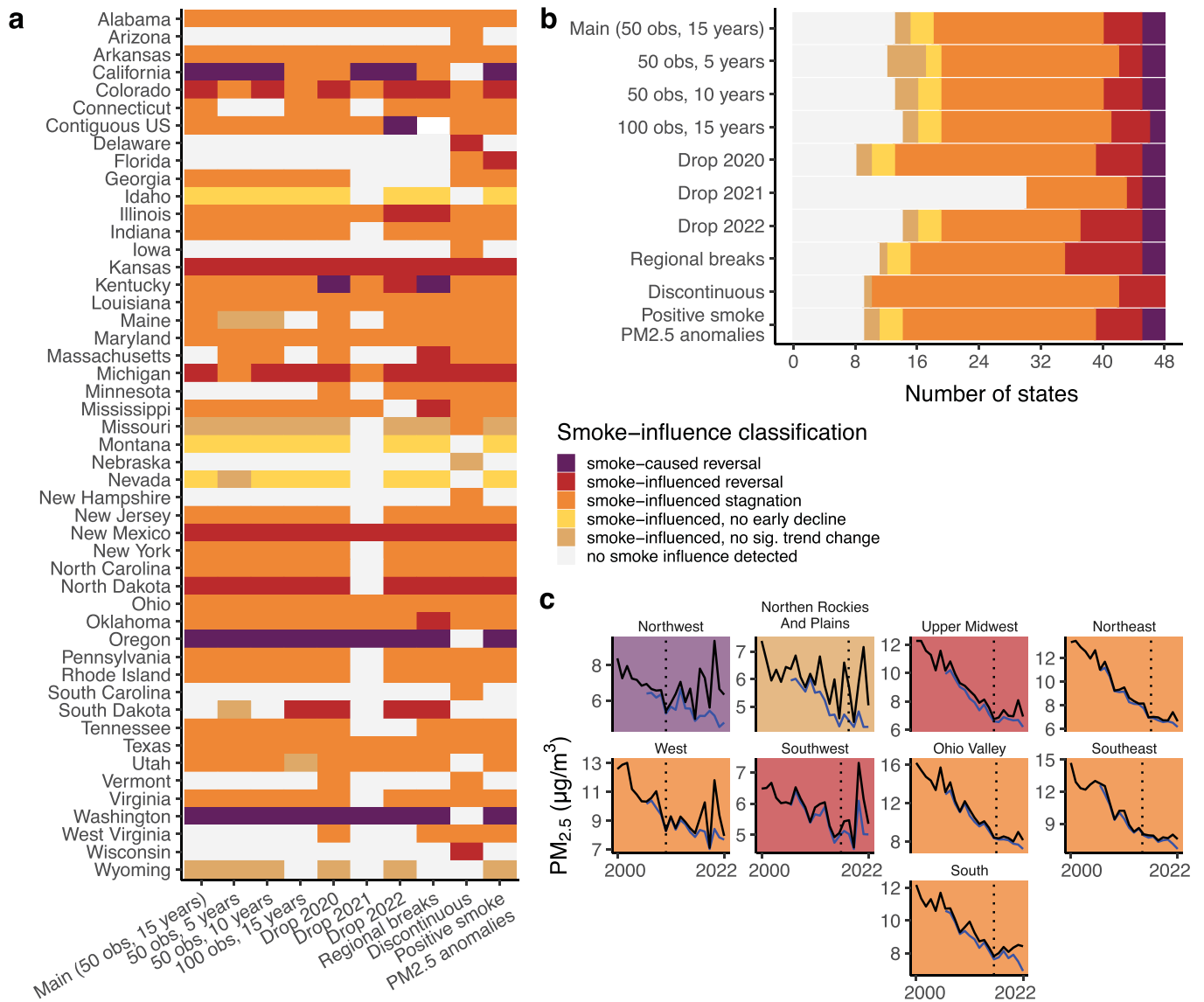
Extended Data Fig. 4 | Sensitivity of estimated differences in slope coefficients used to classify states. Left column shows differences in early (β_1) and recent period (β_2) estimates of changes in total PM_{2.5}, and the confidence interval on estimated differences, that are used to classify states into stagnating/reversing categories. Middle column shows differences in

recent period total PM_{2.5} (β_2) and non-smoke PM_{2.5} (β_2') slopes that are used to classify states as smoke-influenced. Right column shows same, but for recent period changes in extreme days. Colors match sample as denoted in the legend at right.

Article

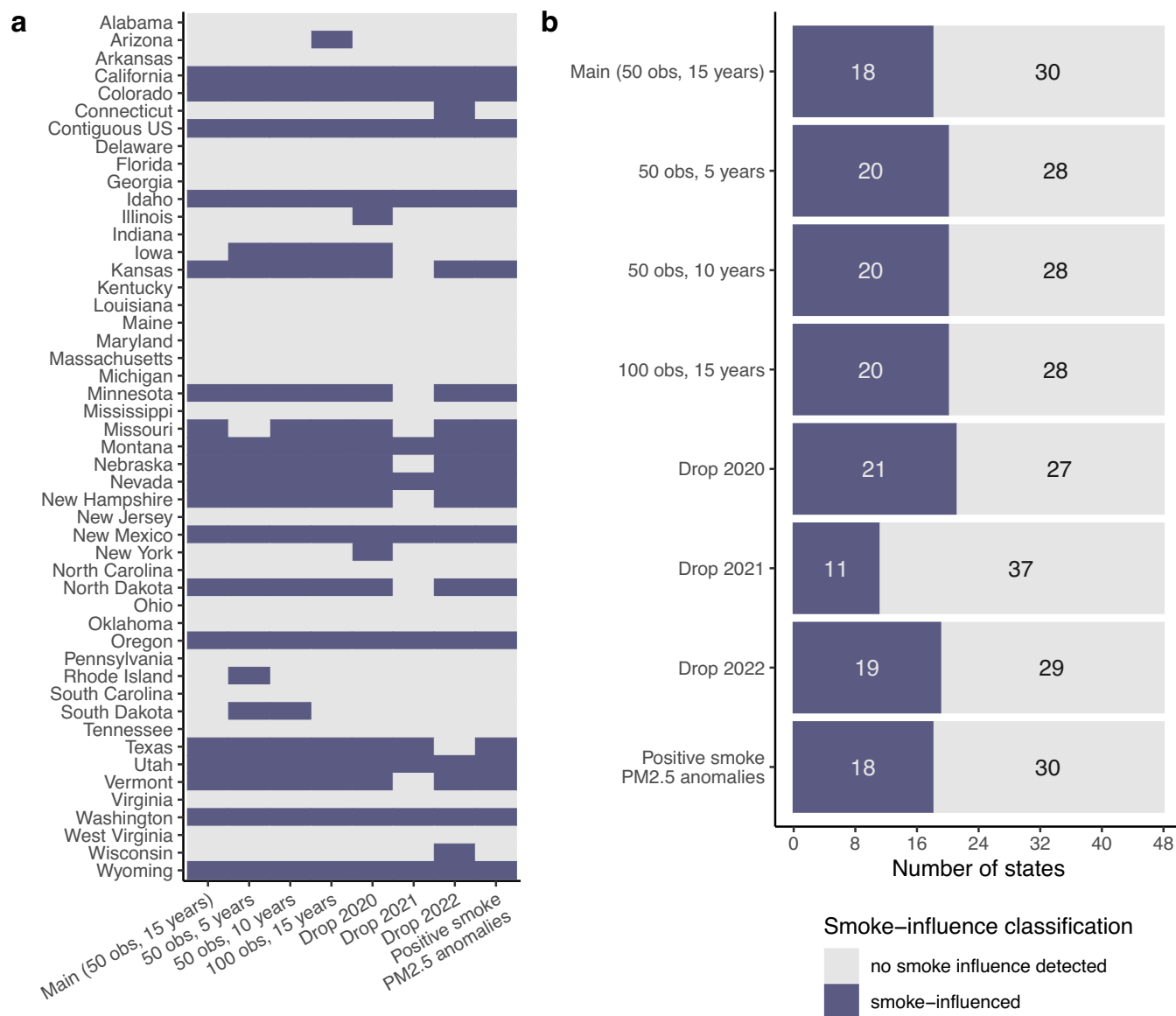


Extended Data Fig. 5 | Sensitivity of total PM_{2.5}-trend classification to different sample restrictions and/or statistical specifications. a. State-specific total PM_{2.5}-trend classification under alternate estimates. **b.** Counts of states in each classification. Model specifications and samples match those in Extended Data Fig. 2.



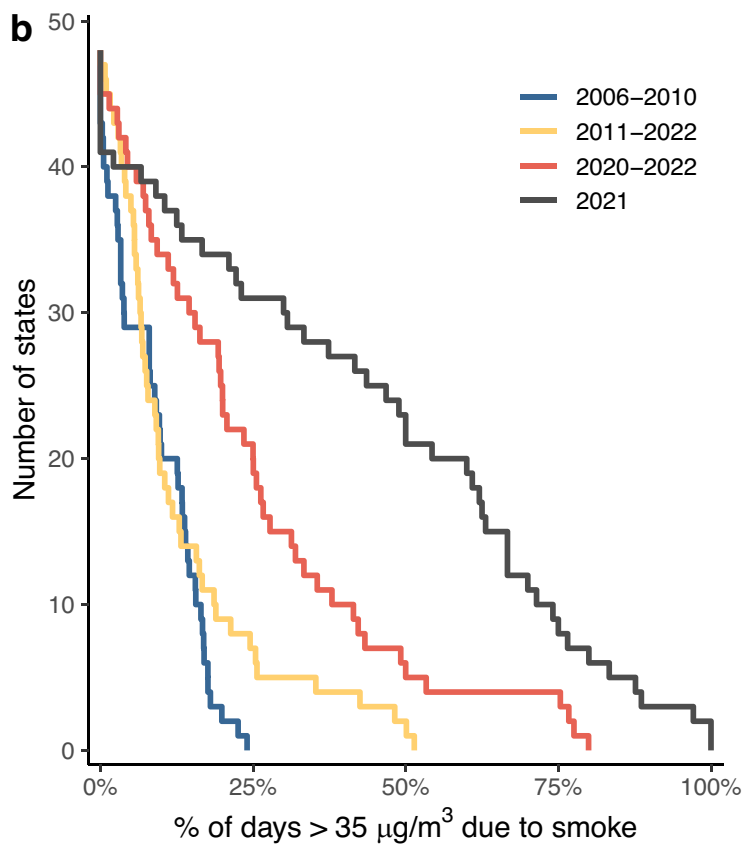
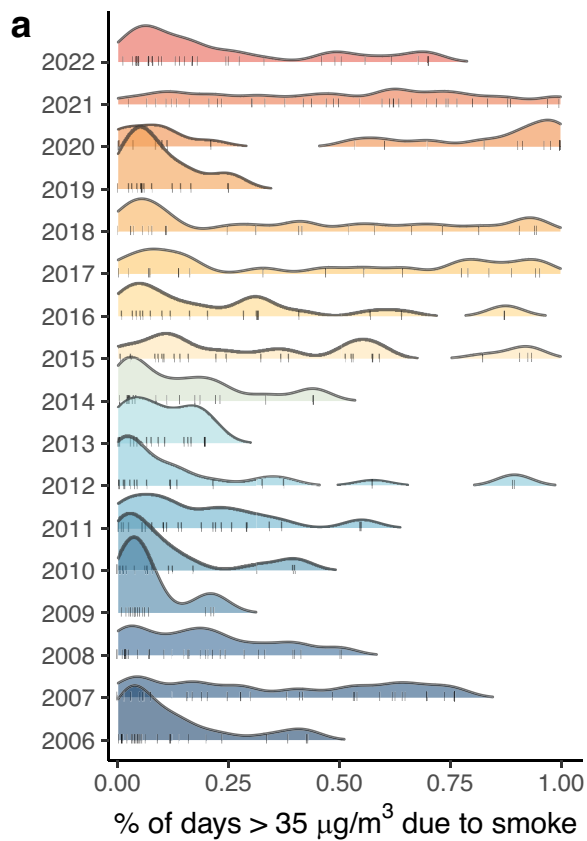
Extended Data Fig. 6 | Sensitivity of smoke-influence classification to different sample restrictions and/or statistical specifications. a. State-specific smoke-influence classification under alternate estimates. **b.** Counts of states in each classification. Model specifications and samples match those in

Extended Data Fig. 2. c. Regional trends in total and non-smoke PM_{2.5}, and regional smoke-influence classifications with region-specific breakpoint estimates (vertical dashed lines).



Extended Data Fig. 7 | Sensitivity of smoke-influence classification on portion of extreme days (> 35 µg/m³) to different sample restrictions.
a. State-specific smoke-influence classification under alternate estimates.

b. Counts of states in each classification. Model specifications and samples match those in Extended Data Fig. 2.



Extended Data Fig. 8 | Distribution of proportion of extreme days due to wildfire smoke by state. **a.** Density plots show, for each year, the distribution across CONUS states of the proportion of days above $35 \mu\text{g}/\text{m}^3$ due to smoke, i.e., days that would have had concentrations $< 35 \mu\text{g}/\text{m}^3$ were smoke not present. Tick marks show values for individual states. **b.** Cumulative distributions of the

number of states where the proportion of extreme $\text{PM}_{2.5}$ days due to wildfire smoke in a time period met or exceeded a given percentage threshold. For instance, the intersection of a vertical line drawn at 50% and each of the depicted lines in the plot would provide estimates of the number of states in each period where at least 50% of extreme days were due to wildfire smoke.

Article

Extended Data Table 1 | Definition of trend groupings

Group	Conditions on slopes				In words
	β_1	β_2	β'_1	β'_2	
Trends in total PM_{2.5}					
Stagnation	< 0	$\leq 0 \ \& \ > \beta_1$			<i>Total PM_{2.5} declined in the first period but declined more slowly or was flat in second period.</i>
Reversal	< 0	> 0			<i>Total PM_{2.5} declined in the first period but increased in the second period.</i>
Influence of smoke PM_{2.5}					
Smoke-influenced Stagnation	< 0	$\leq 0 \ \& \ > \beta_1$		$< \beta_2$	<i>A stagnation where recent period PM_{2.5} would have declined more quickly without smoke.</i>
Smoke-caused Reversal	< 0	> 0		< 0	<i>A reversal where second-period total PM_{2.5} would have declined absent smoke.</i>
Smoke-influenced Reversal	< 0	> 0		$< \beta_2$	<i>A reversal where second period total PM_{2.5} would not have declined absent smoke, but increases would have been at a lower rate.</i>
Smoke-influenced, no early decline	≥ 0			$< \beta_2$	<i>Smoke influenced total PM_{2.5} trends in the second period, but there was no detectable decline in total PM_{2.5} during the first period.</i>
Smoke influence not detected				$\approx \beta_2$	<i>We did not detect an influence of smoke on total PM_{2.5} trends.</i>

We subdivide states into “stagnation” states and “reversal” states based on comparison of trends in total PM_{2.5} between early and recent periods, and then subdivide those based on whether they were smoke-influenced. Coefficients refer to period-specific estimated slopes on PM_{2.5}: β_1 and β_2 are early and recent-period slopes on total PM_{2.5}. β'_1 and β'_2 are corresponding period slopes for non-smoke PM_{2.5}. Strong inequalities (greater or less than) must be statistically significant ($p < 0.05$) for condition to be met.

Extended Data Table 2 | Counts of states in different classifications under different sample restrictions and/or statistical specifications

sample	no smoke influence detected	smoke-influenced	smoke-caused reversal	smoke-influenced reversal	smoke-influenced stagnation	smoke-influenced no trend change	smoke-influenced no early decline
Main (50 obs, 15 years)	13	35	3	5	22	2	3
50 obs, 5 years	12	36	3	3	23	5	2
50 obs, 10 years	13	35	3	5	21	3	3
100 obs, 15 years	14	34	2	5	22	2	3
Drop 2020	8	40	3	6	26	2	3
Drop 2021	30	18	3	2	13	0	0
Drop 2022	14	34	3	8	18	2	3
Regional breaks	11	37	3	10	20	1	3
Discontinuous	9	39	0	6	32	1	0
Positive smoke anom.	9	39	3	6	25	2	3